Highly Precise Determination of Optical Constants and Sample Thickness in Terahertz Time-Domain Spectroscopy

Article *in* Applied Optics · February 1999

DOI: 10.1364/AO.38.000409 · Source: PubMed

3 authors, including:

Lionel Duvillaret
Kapteos
230 PUBLICATIONS **2,316** CITATIONS
SEE PROFILE

Frederic Garet
Université Savoie Mont Blanc
173 PUBLICATIONS **1,761** CITATIONS
SEE PROFILE

Highly precise determination of optical constants and sample thickness in terahertz time-domain spectroscopy

Lionel Duvillaret, Frédéric Garet, and Jean-Louis Coutaz

Time-domain spectroscopy allows fast and broadband measurement of the optical constants of materials in the terahertz domain. We present a method that improves the determination of the optical constants through simultaneous determination of the sample thickness. This method could be applied to any material with moderate absorption and requires only two measurements of the temporal profile of the terahertz pulses: a reference one without the sample and one transmitted through the sample. © 1999 Optical Society of America

OCIS codes: 120.4530, 120.3940, 300.6270.

1. Introduction

Terahertz time-domain spectroscopy is a powerful and a fast technique for measuring the complex refractive index of materials over a wide range of frequency, which extends from a few tens of gigahertz up to a few terahertz.[1] The technique is based on recording the time dependence of the electric field of a short electromagnetic pulse transmitted through a sample. The ratio of the Fourier transforms of the data recorded with and without the sample yields the complex transmission coefficient of the sample in the frequency domain. If a few hypotheses are assumed,[2] the solution of the inverse electromagnetic problem leads easily to the complex refractive index of the sample material. A large number of bulk or thin-film[3] materials such as dielectrics,[4] semiconductors,[5] liquids,[6] and superconductors[7] have already been characterized by use of terahertz spectroscopy.

In this paper we present a method that gives a simultaneous precise determination of the optical constants and the thickness of the sample without requiring any further measurement. We show first in Section 2 that the accuracy of the extracted optical constants critically depends on the uncertainty of the sample thickness and that this accuracy can be improved if the thickness is also determined during the extraction procedure. Our method is as follows: For thick samples the detected echoes of the terahertz signal, which are caused by multiple reflections in the sample, can be time separated well. Therefore the extraction of the optical constants can be performed from a single time-windowed echo. As the effective thickness of material encountered by a single echo varies linearly with the echo number, the effect of any error in the thickness, which is included in the extraction calculation, will be enhanced as the echo number increases. Thus the extracted parameter values will depend on the thickness and on the echo number. For the actual thickness these values will not depend on the echo number. Therefore an examination of the parameter values extracted from different echoes will give the actual value of the sample thickness. This method is presented in Section 3 together with experimental results. For thin samples the echoes are superimposed and cannot be time windowed. Nevertheless, the index and the absorption curves extracted versus the frequency exhibit artificial resonance peaks if the thickness input in the calculation is wrong. These peaks are related to the Fabry–Perot effect. For the actual thickness the peaks disappear. In fact, we show in Section 4 that the peak amplitude varies linearly with the thickness error. Corresponding experimental results are also given.

2. Weights of the Different Error Terms on the Optical Constants' Determination

The accuracy of the extracted optical constants depends on the following factors:

The authors are with the Laboratoire d'Hyperfréquences et de Caractérisation, Université de Savoie, 73376 le Bourget du Lac Cedex, France. L. Duvillaret's e-mail address is duvillaret@univ-savoie.fr.

Received 7 July 1998; revised manuscript received 2 October 1998.

0003-6935/99/020409-07$15.00/0

1. The noise on the temporal profiles of the two terahertz pulses recorded with and without the sample to be characterized.
2. The uncertainty on the sample thickness over the whole surface illuminated by the terahertz beam.
3. The validity of the model that is used to solve the inverse electromagnetic problem.
4. The precision of both the fast Fourier transform's of the temporal profiles and the numerical extraction of the optical constants.

As factor 4 is limited by only the computer's precision, its influence on the accuracy of the optical constants' determination can be made negligible compared with the influence of factors 1–3. Moreover, we[2] previously proposed a method of extraction that is reliable and converges in all practical cases. The influence of factor 1 (noise contribution) is easily quantifiable by calculation of the standard deviation over several records of the terahertz signals. Let us now consider the influence of factor 3, which is the validity of the hypothesis we make to solve the inverse problem.[2] Among all these hypotheses, only the two that follow are not usually satisfied entirely in practice:

- The terahertz beam is supposed to be a plane wave.
- The terahertz beam is assumed to impinge on the sample at normal incidence.

Making a set of several measurements with the removal and the replacement—without a marker—of the sample between two successive measurements allows us to take into account the imperfect orientation of the sample with respect to the direction of propagation of the terahertz beam. Using collimation lenses of a large size to limit the divergence of the terahertz beam for lower frequencies and according to the results obtained by Jepsen *et al.*[8] reveals that the terahertz beam divergence of usual setups is less than 50 mrad for frequencies higher than 200 GHz. For such a beam divergence and if we consider that the terahertz beam is nearly Gaussian, more than 89% of the energy of the terahertz beam propagates in a direction that has an angle of less than 3° with respect to the optical axis. This leads to an error with respect to the extracted parameters of the same order of magnitude as the one induced by sample misorientation.

The influence of the sample thickness on the precision of the extracted parameters (factor 2) is strong and constitutes the main source of error in terahertz time-domain spectroscopy. A typical result, presented in Fig. 1, shows the respective influences of the different factors. The sample is a plate of $LiNbO_3$ whose thickness, as measured with a micrometer, is 1.09 ± 0.01 mm. We are interested in only the optical constants related to the slow optical axis (ordinary axis) of $LiNbO_3$. We distinguish the influence of the uncertainty of the thickness of the sample from the influences of the other factors. These latter influences (factors 1, 3, and 4) were obtained from a

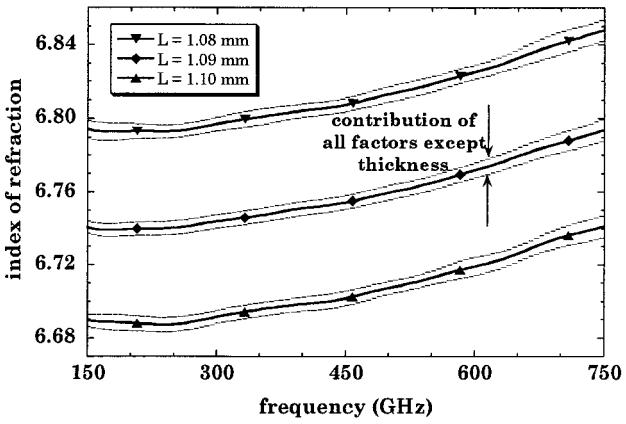

Fig. 1. Extracted ordinary index of refraction of $LiNbO_3$ for different thicknesses (thick curves) together with the standard deviation calculated over 12 records (thin curves).

set of 12 measurements with the sample being removed and replaced between each measurement. As discussed above, the influence of the terahertz-beam divergence should give an error of the same order of magnitude as that given by the noise and the orientation influences. As seen from Fig. 1, the accuracy of the refractive index depends mainly on the precision with which the thickness of the sample is known; therefore it is crucial to determining the thickness of the sample with high precision. A mechanical measurement of the sample thickness is not always possible, and it may not be sufficiently precise. Therefore the best way to maximize the accuracy of the measured refractive index of the sample consists of determining its effective thickness as well. This problem seems to be unsolvable because we have, for each point of frequency, two equations (given by the modulus and the argument of the experimental transmission coefficient) and three unknowns (refractive index, absorption coefficient, and thickness of the sample).

3. Case of Optically Thick Samples

For thick samples the temporal curves exhibit well-separated echoes (see Fig. 2). The basic idea of the method consists of time windowing at least two echoes of the terahertz pulse that are caused by multiple reflections into the sample and to carry out the extraction process for each of these echoes; then we will have more equations than unknowns. This method implies that the absorption of the sample is low enough to allow the existence of a few observable echoes.

For simplicity, let us consider a flat sample placed in air; extension of the method presented here to the general case (a layered sample) is easy but leads to much more complicated expressions. Generally, only the terahertz pulse transmitted directly through the sample is taken into account when determining the complex refractive index. However, any of the other transmitted terahertz pulses that have been subject to multiple reflections in the sample can be

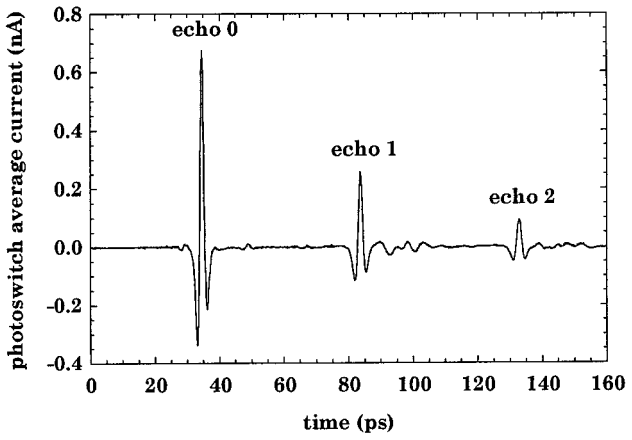

Fig. 2. Terahertz pulses transmitted through a 1.1-mm-thick plate of $LiNbO_3$ with polarization parallel to the slow optical axis (ordinary axis) of the crystal.

taken instead. The complex transmission coefficient $T(\omega)$ (Ref. 2) of the sample for the first transmitted terahertz pulse (echo 0) can easily be extended to the general case of the echo p:

$$T_p(\omega) = \frac{4\tilde{n}_0(\tilde{n}_0 - 1)^{2p}}{(\tilde{n}_0 + 1)^{2p+2}} \times [\exp(-i\tilde{n}_0\omega L_0/c)]^{2p+1} \exp(i\omega L_0/c) = \rho_p(\omega)\exp[-i\phi_p(\omega)], \quad (1)$$

where $\tilde{n}_0 = n_0 - i\kappa_0$ is the complex refractive index of the sample, L_0 is the thickness of the sample, ω is the angular frequency, and c is the speed of light in vacuum. From Eq. (1), we derive the modulus and the argument of $T_p(\omega)$:

$$\rho_p(\omega) = 4({n_0}^2 + {\kappa_0}^2)^{1/2} \frac{[(n_0 - 1)^2 + {\kappa_0}^2]^p}{[(n_0 + 1)^2 + {\kappa_0}^2]^{p+1}} \times \exp[-(2p + 1)\kappa_0 \cdot \omega L_0/c)], \quad (2a)$$

$$\phi_p(\omega) = \frac{[(2p + 1)n_0 - 1]\omega L_0}{c} + 2p \arctan\left(\frac{2\kappa_0}{{n_0}^2 + {\kappa_0}^2 - 1}\right) + \arctan\left[\frac{\kappa_0}{n_0(n_0 + 1) + {\kappa_0}^2}\right]. \quad (2b)$$

The values of n_0 and κ_0 can be extracted from relations (2a) and (2b) by use of numerical codes, as we proposed in Ref. 2. However, the aim of the current paper is to determine the sample thickness together with the optical constants and to supply the reader with analytical expressions that are easy to use. For this purpose, we suppose that the absorption of the material is rather small. Therefore, in relations (2a) and (2b), we can make the approximation $\kappa_0/n_0 \ll 1$. Let us note that this hypothesis directly implies that more than one temporal echo is measurable in the temporal signal. The validity of the method presented in this paper has been checked experimentally in the case of a $LiNbO_3$ crystal (ordinary axis) for which κ_0/n_0 increases with frequency to more than 1% above 600 GHz (absorption of $\sim$15 cm^{-1}).

The expression of the argument of T_p (ω) [Eq. (2b)] is now highly simplified:

$$\phi_p(\omega) \cong [(2p + 1)n_0 - 1](\omega L_0/c). \quad (3)$$

In the present case the index of refraction of the material is extracted directly from expression (3) because the phase $\phi_p(\omega)$ is determined experimentally. The uncertainty of the extracted index of refraction in the first approximation is easily derived from relation (3):

$$\Delta n \cong \left|\frac{1}{(2p + 1)(\omega L_0/c)}\right| \Delta\phi(\omega) + \left|n_0 - \frac{1}{(2p + 1)}\right| \frac{\Delta L}{L_0}, \quad (4)$$

where $\Delta L \ll L_0$ is the error in sample thickness. This error will induce an incorrect value of the extracted index of refraction, which depends on the number p of the echo. In the first order, $\Delta\phi(\omega) = \omega\Delta x/c$, where Δx is the spatial resolution of the delay line used to sample the temporal signals ($\Delta x = c\Delta\tau$, where $\Delta\tau$ is the time resolution of the delay line). The first term on the right-hand side of relation (4) is negligible compared with the second term if $\Delta L \gg \Delta x/[(2p + 1)n_0 - 1]$. This requirement could easily be satisfied in practice, as it depends on the spatial resolution of the delay line. Then, for two different extractions made from two time-windowed echoes p and q taken from the same experimental curve, one will obtain two different approximate refractive indices $n[p]$ and $n[q]$, respectively, whose difference is given by

$$n[p] - n[q] = \{n_0 + \Delta n[p]\} - \{n_0 + \Delta n[q]\} \cong \frac{2(q - p)}{(2p + 1)(2q + 1)} \frac{\Delta L}{L_0}. \quad (5)$$

The error ΔL is thus related directly to the difference $n[p] - n[q]$. Plotting $n[p] - n[q]$ versus ΔL will lead to the actual sample thickness L_0. Relation (5) gives the best precision for L_0 when $(q - p)$ is the largest; this is achieved for $p = 0$ and $q \to +\infty$. Fortunately, by considering just the echoes 0 and 1, we obtain 67% of the maximum difference between $n[p]$ and $n[q]$. Taking more-separated echoes requires recording the signal over a larger temporal window with only a small improvement in the thickness determination. Moreover, when the number of the echo increases its magnitude decreases, and, because of the noise floor, the frequency range over which the refractive index can be extracted is reduced. For these reasons the calculation of ΔL from the difference between the extracted values $n[0]$ and $n[1]$ is the best compromise. From relation (5) we derive

$$\Delta L = \frac{\{n[0] - n[1]\}}{\{n[0] - n[1]\} + 2/3} L, \quad (6)$$

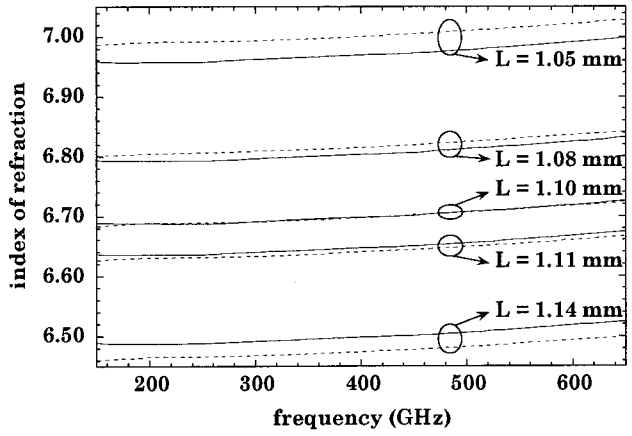

Fig. 3. Ordinary index of refraction of $LiNbO_3$ extracted from echo 0 (solid curves) and echo 1 (dashed curves) for different estimated thicknesses of the sample.

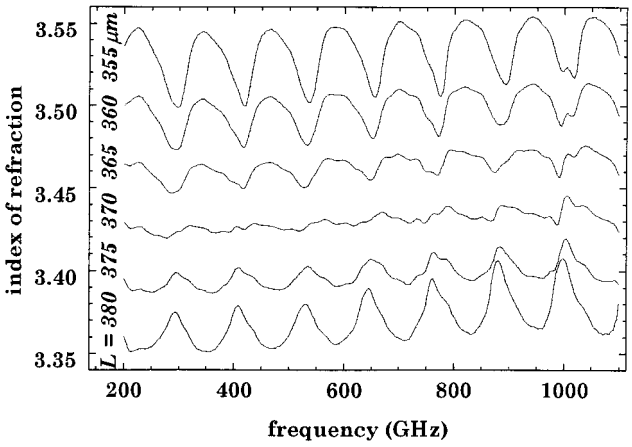

Fig. 5. Index of refraction of silicon for different estimated thicknesses of the sample.

where $L = L_0 + \Delta L$ is the sample thickness used in the extraction of the values of $n[0]$ and $n[1]$. Figures 3 and 4 show an application of these results to the case of the $LiNbO_3$ plate described in Section 2. The extracted indices of refraction for echoes 0 and 1 are represented for different thicknesses over the 150–650-GHz frequency range in Fig. 3. One can see that the difference between the two indices extracted from pulses 0 and 1 increases as the thickness used in the calculation differs from the real thickness. In Fig. 4 we report this difference, $n[1] - n[0]$, averaged over the whole frequency range, versus the thickness L. The best theoretical fit, as derived from expression (5) with L_0 as the unique adjustable parameter, is also represented. The agreement between theory and experiment is very good and leads to $L_0 = 1.100$ mm. A similar agreement, not represented here, is found for the difference $n[2] - n[0]$. Whereas the mechanically measured thickness was 1.09 ± 0.01 mm, the extracted thickness gives a much more precise value of 1.10 (+0.002 or −0.003) mm.

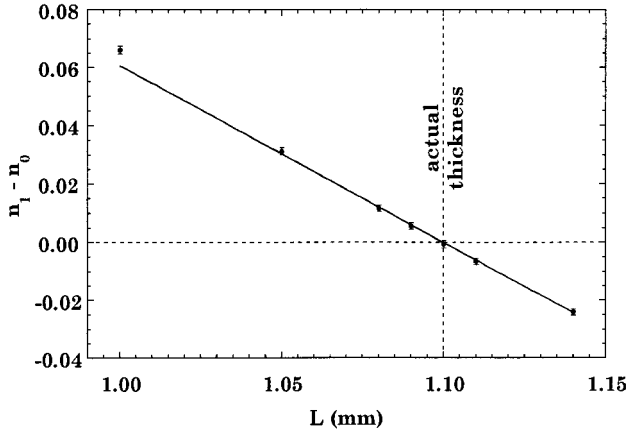

Fig. 4. Difference of the indices of refraction (points with error bars) extracted from echoes 0 and 1, as plotted in Fig. 2, versus the estimated thickness of the sample. The best theoretical fit given by relation (5) and obtained for $L_0 = 1.100$ mm is represented by the solid curve.

In summary, we have demonstrated that the effective thickness of a low-absorption optically thick sample can be extracted, as can its complex refractive index. Moreover, this determination of the thickness is more precise, and, consequently, the index of refraction and the absorption of the material are also more precise. In the present case the uncertainty of the ordinary refractive index of $LiNbO_3$ is reduced by a factor of nearly 4, from 0.055 to 0.015 (2‰)!

4. Case of Optically Thin Samples

In the case of optically thin samples the overlap between successive echoes prevents us from breaking up the terahertz signal transmitted through the sample into its successive echoes. However, the effective thickness of the sample can be extracted from the whole frequency curve. Indeed, when we extract the complex refractive index of the sample by taking a wrong thickness, both the refractive-index and the absorption curves present artificial oscillations versus the frequency. Such oscillations can be seen in Fig. 5, which shows the refractive index of a 368-μm-thick wafer of silicon extracted for different thickness values. Of course, to benefit from the analysis of these oscillations, it is necessary that the refractive-index and the absorption curves must themselves show a smooth frequency behavior. From now on we consider this hypothesis satisfied.

As before, when we consider a flat sample placed in air, its complex transmission coefficient $T(\omega)$ is given by[2]

$$T(\omega; \tilde{n}_0, L_0) = \frac{\dfrac{4\tilde{n}_0}{(\tilde{n}_0 + 1)^2} \exp[-i(\tilde{n}_0 - 1)\omega L_0/c]}{1 - \left(\dfrac{\tilde{n}_0 - 1}{\tilde{n}_0 + 1}\right)^2 \exp(-2i\tilde{n}_0\omega L_0/c)}, \quad (7)$$

where the denominator represents the effect resulting from the back-and-forth reflections in the sample (Fabry–Perot effect). The terms $\tilde{n}_0$ and L_0 are the actual refractive index and the sample thickness, re-

spectively. Any error ΔL in the thickness will induce an error $\Delta\tilde{n}$ in the complex refractive index, but the measured complex transmission coefficient $T(\omega)$ must remain unchanged. So formally we can write

$$T(\omega; \tilde{n}_0, L_0) = T(\omega; \tilde{n}, L), \tag{8}$$

with $\tilde{n} = \tilde{n}_0 + \Delta\tilde{n}$ and $L = L_0 + \Delta L$. Relation (8) leads to

$$\Delta\tilde{n} = (1 - \tilde{n}_0)\frac{\Delta L}{L} - \frac{c}{\omega L}\arg\left[\frac{\dfrac{\tilde{n}_0}{(\tilde{n}_0 + 1)^2}}{\dfrac{\tilde{n}}{(\tilde{n} + 1)^2}}\right] - \frac{c}{\omega L}\arg\left[\frac{1 - \left(\dfrac{\tilde{n} - 1}{\tilde{n} + 1}\right)^2 \exp\left(-2i\tilde{n}\dfrac{\omega L}{c}\right)}{1 - \left(\dfrac{\tilde{n}_0 - 1}{\tilde{n}_0 + 1}\right)^2 \exp\left(-2i\tilde{n}_0\dfrac{\omega L_0}{c}\right)}\right]. \tag{9}$$

The right-hand side of Eq. (9) exhibits three terms. The first term is related to direct propagation through the sample, the second to the transmission coefficient at the two sample surfaces, and the last to the Fabry–Perot effect. As no explicit expression of $\Delta\tilde{n}$ can be derived from Eq. (9), its value can be determined either numerically or by an approximate analytical expression. Such an analytical expression can be obtained in only the approximation of weak absorption (i.e., $\kappa_0/n_0 \ll 1$), as in Section 3. In fact, the first term on the right-hand side of Eq. (9) yields the major contribution to $\Delta\tilde{n}$ (from now on we call it the zero-order value of $\Delta\tilde{n}$). In the present approximation of weak absorption, the second term corresponds to the argument of a real number, and therefore it is null. The third term is only a minor correction to $\Delta\tilde{n}$.[9]

By replacing $\Delta\tilde{n}$ by its zero-order value $(1 - n_0)(\Delta L/L)$ on the right-hand side of Eq. (9), one obtains a more precise estimation of Δn:

$$\begin{aligned}
\Delta n &\cong (1 - n_0)\frac{\Delta L}{L} - \frac{c}{\omega L}\theta,\\
\theta &= \arg\left(\frac{1 - N}{1 - D}\right),\\
N &= \left(\frac{n_0 - 1}{n_0 + 1 + 2\Delta L/L_0}\right)^2 \times \exp\left(-2in_0\frac{\omega L_0}{c}\right)\exp\left(-2i\frac{\omega\Delta L}{c}\right),\\
D &= \left(\frac{n_0 - 1}{n_0 + 1}\right)^2 \exp\left(-2in_0\frac{\omega L_0}{c}\right),
\end{aligned} \tag{10}$$

The first term (right-hand side of line 1) is responsible for the overall shift of the index of refraction extracted with an erroneous sample thickness. The artificial oscillations of the optical constants' curves, plotted versus the frequency (Fig. 5), are due to the second term $c\theta/\omega L$ of line 1 of expression (10). Indeed, two oscillating functions appear in this term, with periods given by

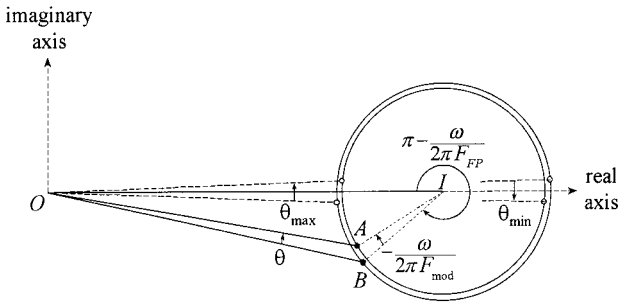

Fig. 6. Representation of the oscillating term $\theta = \arg[(1 - N)/(1 - D)]$, which is responsible for the artificial oscillations of the refractive index seen in Fig. 4 in the complex plane.

$$F_{\mathrm{FP}} = \frac{c}{2n_0L_0}, \qquad F_{\mathrm{mod}} = \frac{c}{2\Delta L}, \tag{11}$$

where F_{FP} is the free spectral range of the sample that behaves like a Fabry–Perot etalon and where F_{mod} depends directly on ΔL. We would like to point out that Δn is studied versus the frequency and therefore F_{FP} and F_{mod} correspond to two different periodicities of the oscillation behavior of Δn in the frequency domain.

Let us carefully analyze the effect of the second term $c\theta/\omega L$ of line 1 of expression (10). This analysis is considerably simplified by use of a representation in the complex plane (see Fig. 6). The vectors **OA** and **OB** represent $1 - N$ and $1 - D$, respectively. The term θ is equal to arg(**OA**) − arg(**OB**) and thus represents the angle between vectors **OA** and **OB**. If it is assumed that $\Delta L \ll L$, points A and B rotate around point I ($|\mathbf{OI}| = 1$, such that $|\mathbf{IA}| = |\mathrm{N}|$ and $|\mathbf{IB}| = |\mathrm{D}|$) with a period close to F_{FP}. As $|N| \cong |D|$, θ oscillates between the extreme values $\theta_{\min}$ and $\theta_{\max}$, as shown in Fig. 6 (note that $\theta_{\min} < 0$). Using elementary geometry in right-angled triangles, one can show that

$$\min(\Delta n) = (1 - n_0)\frac{\Delta L}{L} - \frac{c}{\omega L}\theta_{\max} \cong (1 - n_0)\frac{\Delta L}{L} - \frac{2c}{\omega L}\arctan\left[\frac{R|\sin(\omega\Delta L/c)|}{1 - R}\right], \tag{12a}$$

$$\max(\Delta n) = (1 - n_0)\frac{\Delta L}{L} - \frac{c}{\omega L}\theta_{\min} \cong (1 - n_0)\frac{\Delta L}{L} + \frac{2c}{\omega L}\arctan\left[\frac{R|\sin(\omega\Delta L/c)|}{1 + R}\right], \tag{12b}$$

where

$$R = \frac{|N| + |D|}{2} = \left(\frac{n_0 - 1}{n_0 + 1 + \Delta L/L_0}\right)^2 \cong \left(\frac{n - 1}{n + 1 + \Delta L/L}\right)^2. \tag{13}$$

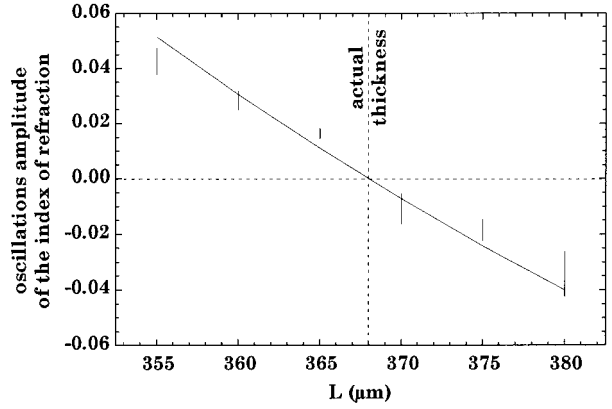

Fig. 7. Amplitude of the oscillations of the extracted refractive indices (error bars), as plotted in Fig. 4, versus the estimated thickness of the sample. The best theoretical fit from relation (15) and obtained for $L_0 = 368$ μm is represented by the solid curve.

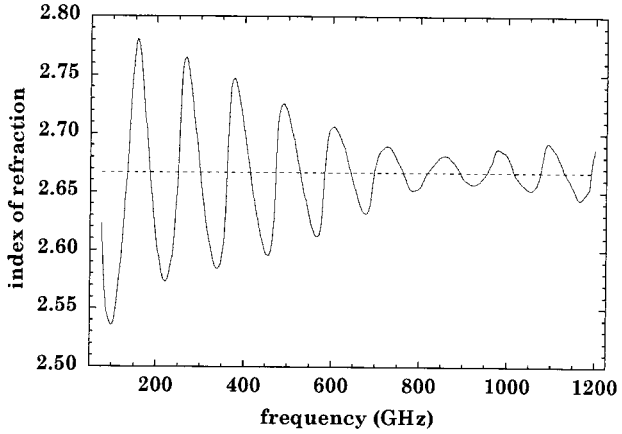

Fig. 8. Extracted index of refraction of silicon for an estimated thickness of the wafer of 540 μm, which is quite different from its actual value of 368 μm.

R takes a value close to the Fresnel coefficient of reflection of the terahertz wave at the air–sample interface. From relations (12), one can easily derive the magnitude of the oscillations of Δn:

$$\mathrm{mag}(\Delta n) = \max(\Delta n) - \min(\Delta n) \cong \frac{2c}{\omega L} \arctan\left[\frac{2R}{1-R^2}\left|\sin\left(\omega \frac{\Delta L}{c}\right)\right|\right]. \quad (14)$$

For angular frequencies much lower than $c/\Delta L$ ($c/\Delta L = 300$ THz for $\Delta L = 1$ μm), one can keep only the first term of the expansion in series of expression (14). Thus the magnitude of the oscillations of the refractive index expresses itself simply as

$$\mathrm{mag}(\Delta n) \cong \frac{4R}{1-R^2}\frac{|\Delta L|}{L}. \quad (15)$$

Let us check experimentally the validity of relations (14) and (15). For the case of the silicon wafer (368 μm thick) represented in Fig. 5, the condition $\Delta L \ll c/\omega$ is satisfied, and, as predicted by relation (15), the magnitude of the oscillations of the refractive index is independent of the frequency. This magnitude (peak to peak), as extracted from Fig. 5, is reported in Fig. 7 versus $L = L_0 + \Delta L$, where L_0 is the actual thickness of the silicon wafer. The best theoretical fit given by relation (15) for the unique adjustable parameter L_0 is also represented. The agreement between theory and experience is very good, despite the presence of noise in the curves of Fig. 5, and leads to the actual wafer thickness of $L_0 = 368$ μm.

Even if we start with a very large error ΔL, relation (14) leads directly to the actual thickness of the sample. As an example, Fig. 8 shows the extracted refractive index of silicon for $\Delta L = 172$ μm (error of ~50%). Next, in Fig. 9 we report the magnitude of the oscillations observed in Fig. 8 versus the frequency, together with the best theoretical fit obtained for $L_0 = 368.5$ μm. One can note the excellent agreement between the theoretical fit and the experimental points. Moreover, the magnitude of the oscillations is approaching null for $\sin(\omega\Delta L/c) = 0$ [see relation (14)], i.e., for a frequency of $f = F_{\mathrm{mod}}$, which is equal to 872 GHz in the present case.

To demonstrate the sensitivity of the method for the determination of thickness, we also plotted in Fig. 9 two other theoretical curves, calculated for $L = 368.5 \pm 7.5$ μm. It appears very clearly that these two theoretical curves do not fit the experimental data. So, even with an error close to 50% of the sample thickness, we are able to determine the actual thickness of the sample with a precision of a few micrometers, i.e., less than 1%! For the three theoretical curves shown in Fig. 9, a vertical offset of 0.01 was applied to take into account the weak residual oscillations (magnitude of 0.01) of the refractive index that persist even for the actual value of $L_0 = 368$ μm. The period of these residual oscillations, which is equal to the free spectral range F_{FP}, clearly indicates the presence of an experimental artifact. This arti-

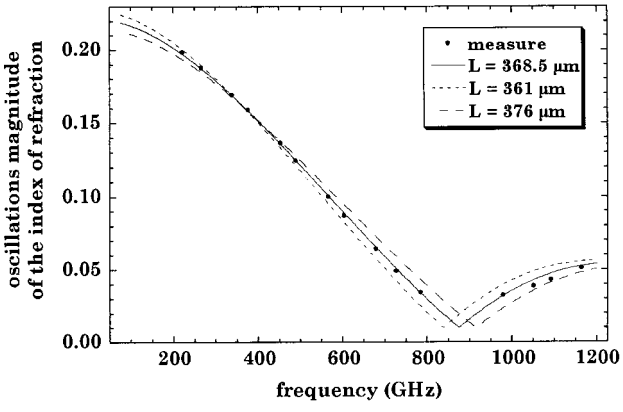

Fig. 9. Magnitude of the oscillation of the index of refraction of silicon (points), as plotted in Fig. 7, versus the frequency. Three theoretical fits given by relation (14) for three different values of the thickness are also represented.

fact could be attributed to a weak lack of parallelism of the sample.

5. Conclusion

We have presented a novel, to our knowledge, method for improving the determination of optical constants in terahertz time-domain spectroscopy. This method, which applies to any material of low absorption, allows us to determine the thickness of the sample with great accuracy (better than 1%). Thus the sample-thickness error, which is often the major source of uncertainty for the determination of optical constants, is minimized. Therefore the refractive index is obtained with enhanced precision ($\Delta n \approx 10^{-2}$ for a sample thickness of $L_0 \approx 1$ mm). This method can be applied not only to terahertz time-domain spectroscopy but also to any kind of optical constant measurement in the time domain.

References and Notes

1. See, for example, the special issue on terahertz electromagnetic pulse generation, physics, and applications, J. Opt. Soc. Am. B **11**(12), (1994).
2. L. Duvillaret, F. Garet and J.-L. Coutaz, "A reliable method for extraction of material parameters in THz time-domain spectroscopy," IEEE J. Select. Topics Quantum Electron. **2,** 739–746 (1996).
3. S. Labbé-Lavigne, S. Barret, F. Garet, L. Duvillaret, and J.-L. Coutaz, "Far-infrared dielectric constant of porous silicon layers measured by THz time-domain spectroscopy," J. Appl. Phys. **83,** 6007–6010 (1998).
4. D. Grischkowsky, S. Keiding, M. van Exter, and Ch. Fattinger, "Far-infrared time-domain spectroscopy with terahertz beams of dielectrics and semiconductors," J. Opt. Soc. Am. B **7,** 2006–2015 (1990).
5. M. van Exter and D. Grischkowsky, "Optical and electronic properties of doped silicon from 0.1 to 2 THz," Appl. Phys. Lett. **56,** 1694–1696 (1990).
6. J. E. Pedersen and S. R. Keiding, "THz time-domain spectroscopy of nonpolar liquids," IEEE J. Quantum Electron. **28,** 2518–2522 (1992).
7. J. F. Whitaker, F. Gao, and Y. Liu, "THz-bandwidth pulses for coherent time-domain spectroscopy," in *Nonlinear Optics for High-Speed Electronics and Optical Frequency Conversion*, N. Peyghambarian, R. C. Eckhardt, and D. D. Lowenthal, eds., SPIE **2145,** 168–177 (1994).
8. P. U. Jepsen and S. R. Keiding, "Radiation patterns from lens-coupled THz antennas," Opt. Lett. **20,** 807–809 (1995).
9. We showed in Ref. 2 that the Fabry–Perot effect can be treated as a perturbation for the extraction of the complex refractive index of the sample in all practical cases.